minerals

MDPI

Article

Ore Mineralogy and Typomorphism of Native Gold of the Spokoininsky Cluster of the Aldan–Stanovoy Gold Province

Larisa A. Kondratieva *, Galina S. Anisimova and Veronika N. Kardashevskaia

Diamond and Precious Metal Geology Institute, SB RAS, 677000 Yakutsk, Russia;
gsanisimova1952@mail.ru (G.S.A.); kardashevskaya92@mail.ru (V.N.K.)
* Correspondence: lkon12@yandex.ru; Tel.: +7-4112-33-58-72

Abstract: The ore mineralogy of a new promising target of the Aldan–Stanovoy gold province—the Spokoininsky cluster—is considered. Gold mineralization is represented by a volumetric, nonlinear type, unconventional for the region; it is related to elements of fold structures and reverse fault in the enclosing metamorphic basement rocks. Vein-disseminated sulfide–(pyrite)–quartz ores build up deposit-like bodies in beresites from gneisses and granite gneisses and are associated with Mesozoic igneous rocks of subalkaline formations. Mineralization is characterized by polysulfide (Fe-Cu-Pb); gold–bismuth (Au-Bi) and gold–silver–telluride (Au-Ag-Te) mineral types. Different mineral types have their own typomorphic minerals and typochemistry (fineness and impurities) of native gold. The widespread distribution of telluride mineralization and its great importance in the formation of gold mineralization on the Aldan shield is confirmed. The distribution area of bismuth (including tellurium–bismuth) mineralization in the southern part of the Aldan shield, in the zone of influence of the Stanovoy deep fault, has been identified.

Keywords: gold mineralization; metasomatites; bismuth; tellurides; uytenbogaardtite; bismoclite; cervelleite; native gold; supergene gold; the Spokoininsky cluster; the Aldan-Stanovoy gold province; the Aldan shield

check for updates

Citation: Kondratieva, L.A.; Anisimova, G.S.; Kardashevskaia, V.N. Ore Mineralogy and Typomorphism of Native Gold of the Spokoininsky Cluster of the Aldan–Stanovoy Gold Province. *Minerals* **2023**, *13*, 543. https://doi.org/10.3390/min13040543

Academic Editor: Huan Li

Received: 16 March 2023
Revised: 8 April 2023
Accepted: 10 April 2023
Published: 12 April 2023

1. Introduction

The Spokoininsky ore cluster is a new promising ore target of the Aldan-Stanovoy gold province (ASGP), identified during prospecting in 2020 [1]. The search for ore targets has been undertaken since the 1970s [2] but resulted in only scattered mineralization points with an unclear structural position and mineralogy of ores. The territory of the cluster occupies the upper reaches of the right tributary of the Timpton river—the Ulakhan-Tarakanda River (Bol. Tyrkanda)—and covers the most productive southeastern part of the Tyrkanda gold-rich area, known since the beginning of the last century for rich placers of gold, from which more than 20 tons of gold were extracted. The primary sources of gold feeding the placers have not yet been identified. The largest placer deposit of the region is the placer of the Bol. Tyrkanda River, with gold reserves of more than six tons, which is in development to this day [3]. The placer deposit is localized in the valley of the river, starting near the mouth of the Spokoiny Creek, i.e., the Spokoininsky cluster.

The first mineralogical studies of the Spokoininsky cluster ores revealed a variety of Bi, Te, and Ag minerals, as well as a number of rare minerals, such as bismoclite and uytenbogaardtite. Determination of the connection of gold with certain mineral associations and the comparative analysis of morphological and geochemical properties of native gold of primary ores and supergene gold of eluvial deposits are relevant tasks for understanding the factors of its formation, i.e., the ore genesis.

2. Materials and Methods

Materials used for our research are 72 hand-sampled specimens of primary ores taken from surface mine workings and outcrops, as well as 20 shallow-pit samples from loose detrital clay material of eluvial deposits.

The polished sections made from the samples were optically examined using a Jenavert ore microscope in reflected light. The minerals were analyzed on a Camebax-micro X-ray spectral microanalyzer and a JEOL JSM-6480LV scanning electron microscope with an OXFORD energy spectrometer, and the Back Scattered Electron images were taken at the Diamond and Precious Metal Geology Institute, Siberian Branch, Russian Academy of Sciences (Yakutsk, Russia). The quantitative analysis was carried out using Software INCA Energy (Version 4.17, Oxford Instruments, Abingdon, Oxfordshire, UK) with XPP matrix correction scheme developed by Pouchou and Pichoir. Operating conditions were 20 kV voltage, a beam current of 1.08 nA, a beam diameter of 1 mm, and measurement time of 10 s. Analytical lines: Bi, Au−M; Te, Pb, Ag, Sb, S–L; and Cu, Fe, Zn, S–K. Standards: gold 750–Au, Ag, Bi_2S_3–(bismuthinite)–Bi, HgTe (coloradoite)–Hg, Te, $CuSbS_2$ (chalcostibite)–Cu, Sb, S, ZnS (sphalerite)–Zn, $CuFeS_2$ (chalcopyrite)–Fe, PbS (galena)–Pb, and FeAsS (arsenopyrite)–As. Element detection limits (wt.%) for the X-ray spectral microprobe analyses: Au 0.145, Ag 0.078, As 0.129, Hg 0.137, Cu 0.057, Fe 0.032, Pb 0.076, Bi 0.108, Sb 0.044, and Zn 0.074. Limits of element detection (wt.%) scanning electron microscope equipped with energy spectrometer: Au 1.84, Ag 0.96, Hg 1.6, Cu 1.22, Fe 1.04, Pb 1.78, and Bi 2.7.

3. Geology of the Spokoininsky Cluster

The Spokoininsky cluster is located on the northern slope of the Aldan shield. The territory is characterized by a large depth of the erosion section—the Archean crystalline basement—composed of gneisses and crystalline schists of the Sutamskaya and Kyurikanskaya formations of the Dzheltula series of the Lower Archean, which is exposed throughout the area of the region. The basement rocks are migmatized and contain concordant and transverse bodies of the Archean and Proterozoic granites, ultrabasites, gabbro-diorites, and gabbro-diabases.

The territory is located in the zone of the regional Tyrkanda fault, which has a north–northwestern strike and a thickness of up to 10–15 km. During the Mesozoic tectonic–magmatic events, the Tyrkanda fault zone underwent destruction: the northeastern seams of the extended faults of the Sunnaginskaya system are superimposed on it, which are a reflection of the global North Stanovoy fault located to the south.

The position at the intersection cluster of regional faults determines the intense fault tectonics and magmatism of the Mesozoic activation stage. The Mesozoic igneous rocks are represented by fields of dikes, small stocks, folded rocks of monzonite–syenite, and alkaline–syenite formations. The formation of intrusions involved contact–metasomatic and hydrothermal–metasomatic processes in the form of hornfelsing, chloritization, epidotization, sericitization, and silification of host rocks. The Spokoininsky ore cluster is located within the Mayskaya synclinal structure composed of amphibole and biotite–amphibole gneisses, with interlayers of bipyroxene and diopside gneisses.

The most promising ore fields are Spokoinoe and Mayskoe (Figure 1). The Spokoinoe ore field is located on the left bank of the lower reaches of the Spokoiny creek in the northern part of the cluster, and Mayskoe field covers the watershed of the Spokoiny, Maysky, and Taborny creeks in the south.

The Spokoinoe ore field is confined to the periclinal closure of the Mayskaya synclinal structure, where slight granitization of gneiss is noted. Gneisses are injected by the Early Proterozoic granitoids and intruded by bodies of the Mesozoic igneous rocks (nordmarkites, syenite porphyries, hornblende and biotite porphyries, minettes, spessartites, and vogesites), forming stock-shaped deposit bodies, dikes, and lenticular bodies with sharp swells, confined to the axial parts of complex folds.

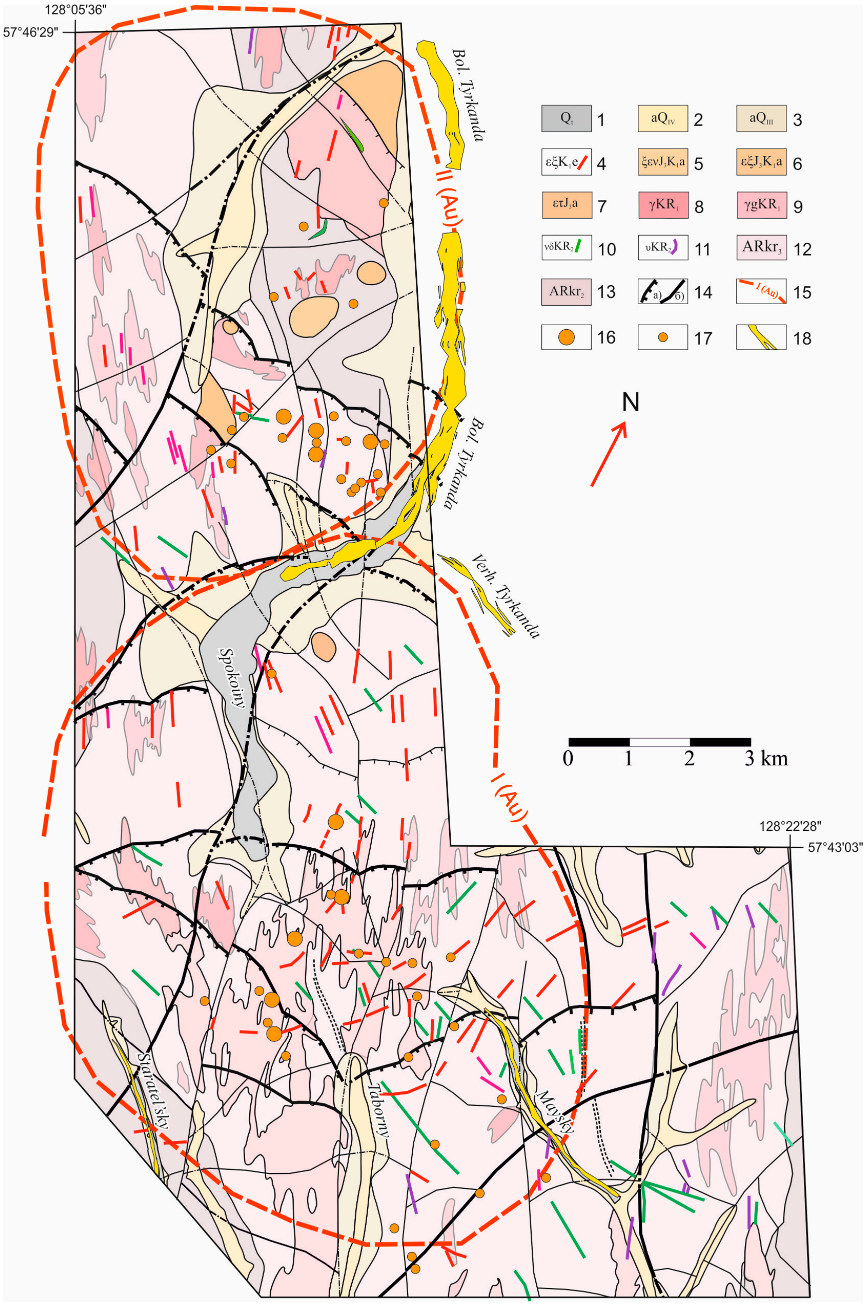

Figure 1. Schematic map of geological structure of the Spokoininsky ore cluster [1] with changes: 1—technogenous formations: rewashed deposits of prospectors polygons; 2—Quaternary: channel and low floodplain alluvium; 3—Upper Quaternary deposits: floodplain, channel, above-floodplain terrace alluvium, and fluvioglacial deposits; 4—dikes of alkaline and alkaline–earth syenites; 5–7—stocks: 5—alkaline–earth syenite, 6—pulaskites, laurvikites, and nordmarkites, 7—alkaline trachytes; 8—biotite, muscovite, and garnet granites, hypersthene–amphibole microcline granites, enderbites, and granites undivided; 9—variously hybridized granitized rocks and granite gneisses; 10—biotite, muscovite, and garnet granites, hypersthene–amphibole microcline granites, enderbites, and granites undivided; 11—variously hybridized granitized rocks and granite gneisses; 12,13—Kurikan Formation: 12—upper subformation (hypersthene and biotite–hypersthene gneisses and crystal schists); 13—middle subformation (biotite–hypersthene and two-pyroxene gneisses and crystal schists); 14—faults: a—reverse (to thrust) faults controlling distribution of highly promising anomalous geochemical fields and b—other faults; 15—ore fields: I (Au)—Mayskoe and II (Au)—Spokoinoe; 16—gold primary occurrences; 17—shallow-pit samples containing free gold; 18—gold placer deposits.

Faults belong to the systems of the Tyrkanda fault: strike-slips, strike-slip reverse faults of the northwestern strike, and the Sunnaginsky fault: normal faults, reverse faults of the northeastern strike. The gentle strippings of the latitudinal and sublatitudinal strikes, characterized as overthrust reverse faults, are less manifested. The latitudinal and northwestern directions within the ore field are well expressed by gold anomalies forming a discrete band, most contrasting at the intersection with the structures of the Sunnaginsky fault.

Gently dipping (10–20°) zones of schistosity of latitudinal and sublatitudinal strike contain gold ore bodies and are transverse, sub-concordant to the general occurrence of gneiss (Figure 2). Morphologically, ore bodies form gently dipping lenticular-ribbon-like deposits in the zones of schistosity, with a wavy surface, alternating with each other echelon-like in the latitudinal direction when wedging out along the strike. Dip angles are gentle, from less than 10° to 30°, and infrequently, 40°. The general azimuth of the dip is to the north. The thickness of individual deposits exposed by ditches ranges from 0.1–0.5 m to 1.6–2.5 m.

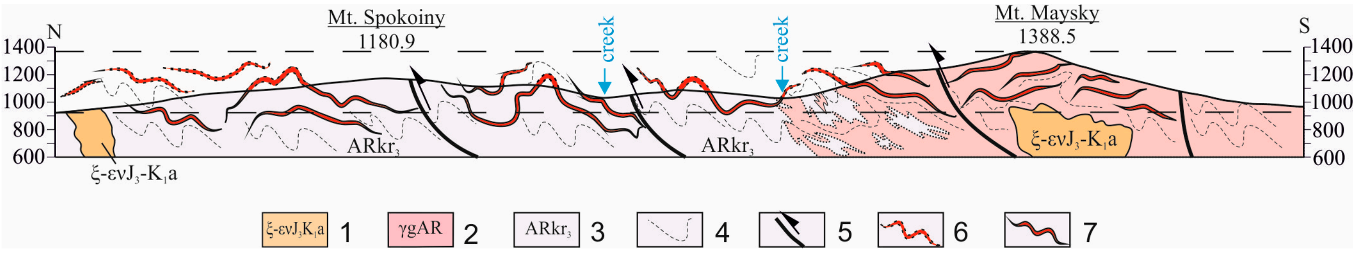

Figure 2. Geological cross section for gold mineralization of the Spokoininsky ore cluster, longitudinal section [1] with changes: 1—stocks of alkaline syenites; 2—granitized gneisses and granite gneisses; 3—Kurikan Formation, upper subformation; 4—folds; 5—reverse (to thrust) faults; 6,7—lodes: a—eroded and b—not eroded.

In contrast to the Spokoinoe ore field, the Mayskoe field is characterized by a significantly higher degree of granitization, especially in the southern, most elevated part of the site and the absence of large outcrops of the Mesozoic igneous rocks. The Mesozoic magmatism occurs in the form of frequent dikes, dike-like bodies of syenite porphyries, and lamprophyres, filling the faults of the northwestern and northeastern strike. In the northern, more eroded part of the ore field, a stock-shaped intrusion of alkaline–earth syenites has been exposed, and due to the presence of high-contrast magnetic anomalies, similar unexposed bodies are assumed in the south.

The correlation of the Mesozoic magmatic formations and gold mineralization is well demonstrated at the Mayskoe field. In the northern part of the site, ore zones are exposed by ditches in contact with the bodies of syenite porphyries and lamprophyries, which are also slightly gold-bearing. In the south are geochemical anomalies of gold trace unexposed intrusions. The main role as an ore-controlling factor also belongs to gentle structures, such as overthrust reverse faults of the latitudinal and sublatitudinal strike. Another important factor is the presence of plicative structures complicating the Mayskaya syncline. Ore mineralization is localized in areas of schistosity, with cleavage confined to various elements of folds, bends of hinges, turns of limbs, and other complicating elements (Figure 2). Ore bodies form gently and steeply dipping lenticular-ribbon-like deposits, bodies of complex shape in the zones of schistosity, with dip angles from 10–20° to 70°. Ore intervals with gold mineralization are 2.0–5.0 m and 7.0–10.0 m. In the identified ore intervals with a gold content, increased Cu contents are recorded (500–5000 g/t), Pb (100–200 g/t), Bi (50–100 g/t), and Ag (60–200 g/t) [1].

In general, a model of gold mineralization of a volumetric, nonlinear type related to elements of plicative structures and reverse fault tectonics in the host-granitized metamorphic rocks of the basement is proposed for the Spokoininsky ore cluster, represented by a combination of deposit-like bodies with vein-disseminated sulfide–(pyrite)–quartz type of mineralization. Mineralization is localized in beresites from gneisses and granite gneisses with vein-disseminated pyrite–quartz gold mineralization and is associated with the Mesozoic igneous rocks of subalkaline formations.

Considering structural features, brecciated, vein–veinlet, and disseminated types of ores are common. The main vein mineral is quartz—white, grayish, rarely honey-yellow, sometimes transparent, opaline silica, fine crystalline, drusoid, massive and brecciate, and chalcedonic in thin veinlets. It forms veinlets, lenses, geodes, and small net-shaped veinlets in beresites and beresitized gneisses, with thicknesses from 0.5 mm to 1.0–15.0 cm.

4. Results

4.1. Mineralogy of Ores

Mineralization of the Spokoininsky gold ore cluster is characterized by the following mineral types: polysulfide (Fe-Cu-As-Pb-Zn), gold–bismuth (Au-Bi), and gold–silver–telluride (Au-Ag-Te) (Table 1).

Table 1. Typification of the ores of the Spokoininsky cluster.

Type of Ore	Minerals
Polysulfide	Pyrite, chalcopyrite, galena, arsenopyrite, sphalerite, native tin, scheelite, and wolframite
Gold–bismuth	Native bismuth, bismuthite, tellurobismuthite, bursaite, matildite, cuprobismutite, smirnite, and bismoclite
Gold–silver–telluride	Krennerite, sylvanite, petzite, hessite, cervelleite, polybasite, native silver, acanthite, and uytenbogaardtite

The polysulfide mineral type is widespread in the area of the ore cluster. The main ore mineral is pyrite. The mineral—to varying degrees oxidized, often large, cubic, and pentagon dodecahedral, and up to 1.0 cm across—grows on quartz druse crystals. Fine-grained pyrite, more often oxidized, forms concentrations, with massive veinlets up to 0.5 cm thick at the base of quartz druses and host beresites. Pyrite is often a matrix for ore microminerals. Chalcopyrite occurs as allotriomorphic particles in quartz and pyrite. All other minerals are micron-sized. Galena forms frequent small particles, represented by thin rounded and irregular shapes. Hypidiomorphic microcrystals (<10 microns) of arsenopyrite are sporadically observed. Sphalerite is rare, characterized by a Fe content of up to 12%.

The ores contain very few grains of native tin, scheelite, and wolframite. Native tin and wolframite form small 10–15 micron interstitial grains in metasomatic quartz and scheelite—oval-rounded and isometric inclusions in pyrite and iron hydroxides replacing pyrite.

Typomorphic minerals of gold–bismuth mineral type are native bismuth, bismuthite (BiS), tellurobismuthite (Bi_2Te_3), bursaite ($Pb_5Bi_4S_{11}$), cuprobismutite ($Cu_8AgBi_{13}S_{24}$), and matildite ($AgBiS_2$) (Figure 3, Table 2). Secondary minerals are represented by smirnite (Bi_2TeO_5) and bismoclite (BiOCl). Bismuth mineralization was identified mainly in ores of the Mayskoe ore field. Tellurobismuthite forms elongated and oval crystals in pyrite, and bursaite forms tabular crystals in quartz. Native bismuth in growth with matildite is enclosed in pyrite. They also revealed matildite with a significant content of Te (7.11 wt.%) as well as an obscure oxygen-containing phase with a spongy surface in which the concentration of Te reached 23.25 wt.%. Cuprobismutite and smirnite were observed in supergene gold: smirnite is represented by a disintegrated mass in the form of a border and cuprobismutite in relic grains. Among the bismuth minerals, matildite and bismoclite were found in the Spokoinoe ore field. Matildite was observed in supergene gold in close growth with galena in the form of a border and had microinclusions in it. Bismoclite is a secondary mineral of bismuth, found in a quartz cavity in the form of a tetragonal crystal with faces truncated at 45°.

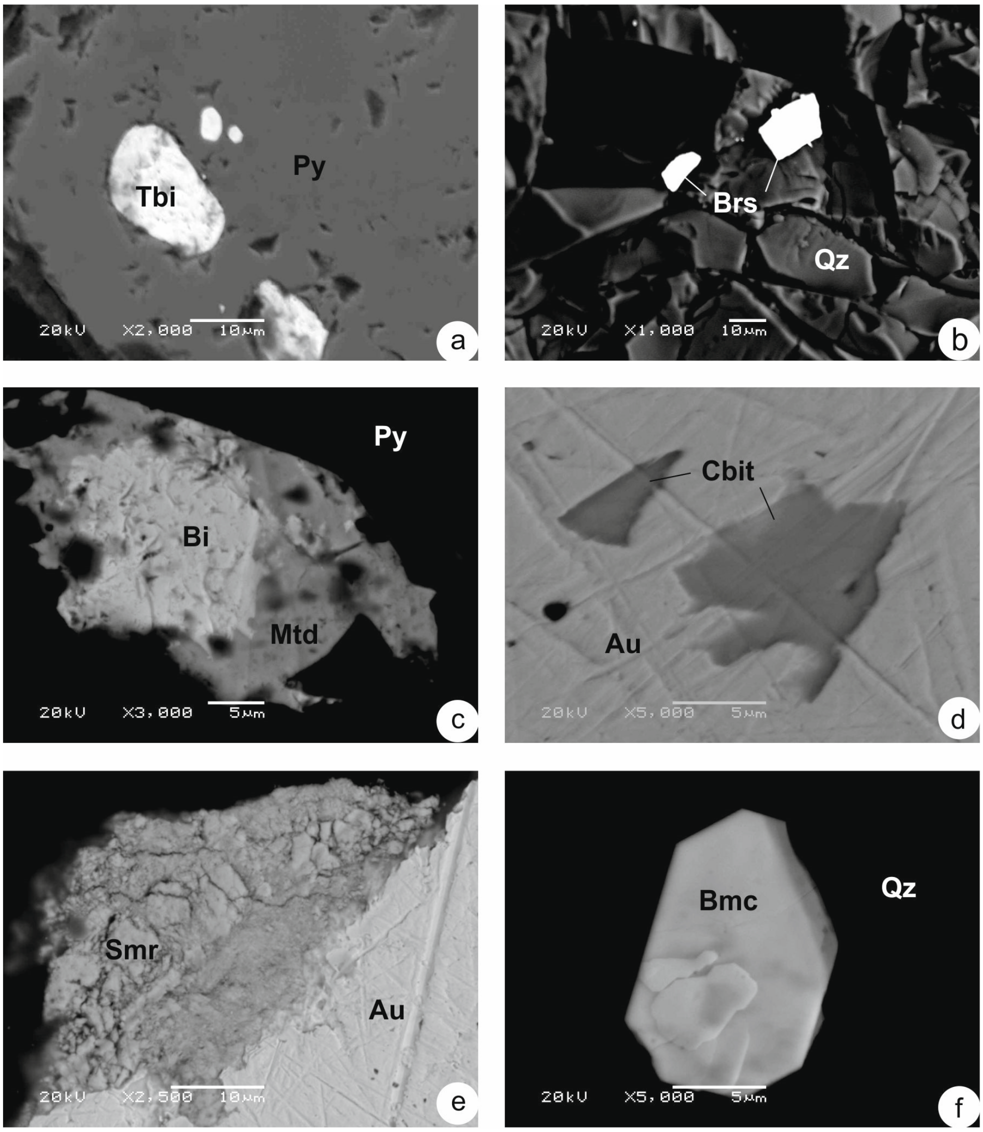

Figure 3. Gold–bismuth mineralization of the Spokoininsky ore cluster: (**a**)—ellipsoidal grains of tellurobismuthite (Tbi) in pyrite (Py), (**b**)—tabular grains of bursaite (Brs) in quartz (Qz), (**c**)—native bismuth (Bi) in growth with matildite (Mtd) in pyrite (Py), (**d**)—relics of cuprobismutite (Cbit) in supergene gold (Au), (**e**)—disintegrated mass of smirnite (Smr) on the edge of supergene gold (Au), (**f**)—bismoclite crystal (Bmc) in quartz (Qz).

Table 2. Chemical composition of bismuth minerals (in wt.%).

Mineral	Bi	Te	Ag	Cu	Cl	Pb	S	Si	Fe	O	Total	apfu
Native Bi	100.33										100.33	$Bi_{1.00}$
Tellurobismuthite	51.43	47.89									99.32	$Bi_{1.96}Te_{3.00}$
Bismuthite	81.50						17.51				99.01	$Bi_{2.13}S_{3.00}$
Bursaite	36.63		3.96			44.92	14.41				99.92	$(Pb_{5.31}Bi_{4.27}Ag_{0.90})S_{11.00}$
Matildite	56.32		27.09				15.33				98.75	$Ag_{1.05}Bi_{1.12}S_{2.00}$
Cuprobismutite	60.36		4.95	12.28			16.34				93.93	$(Cu_{9.10}Bi_{13.54}Ag_{2.16})S_{23.00}$
Bismoclite	71.59				11.87			2.00	2.13	11.55	99.13	$Bi_{1.02}Fe_{0.11}Si_{0.21}Cl_{1.00}$
Smirnite	66.79	19.13							1.86	12.38	100.16	$Bi_{2.06}Te_{0.97}Fe_{0.22}O_{5.00}$

Bismuth minerals are characterized by the presence of a significant impurity of silver (3.96 wt.%) in bursaite and cuprobismutite (4.95 wt.%). Impurities of Fe and/or Si in the composition of the bismoclite and smirnite are due to the influence of the background matrix of quartz and iron hydroxides. There is also a background impurity of iron in smirnite.

Gold–silver–telluride type is represented by krennerite ($AuTe_2$), sylvanite ($(Au,Ag)_2Te_4$), petzite (Ag_3AuTe_2), hessite (Ag_2Te), cervelleite (Ag_4TeS), polybasite, native silver, acanthite (Ag_2S), and uytenbogaardtite (Figure 4, Table 3). The grain size does not exceed 50 microns. In addition, gold bismuth type is more developed in the Mayskoe ore field. Minerals of petzite–hessite paragenesis and polybasite are observed in the form of oval and irregular grains in pyrite. Tellurides of the krennerite group were observed as inclusions in hessite and petzite, gravitating towards the central parts of the grains. There are cases of hessite growths with tellurobismuthite. Acanthite, native silver, and uytenbogaardtite are observed in the ores of the Spokoinoe field, and hessite–cervelleite paragenesis is developed in the form of rounded micron inclusions (no more than 30 microns) in hypergene gold. Along with cervelleite of stoichiometric composition, there is cervelleite with a considerable content of copper up to 5.92%.

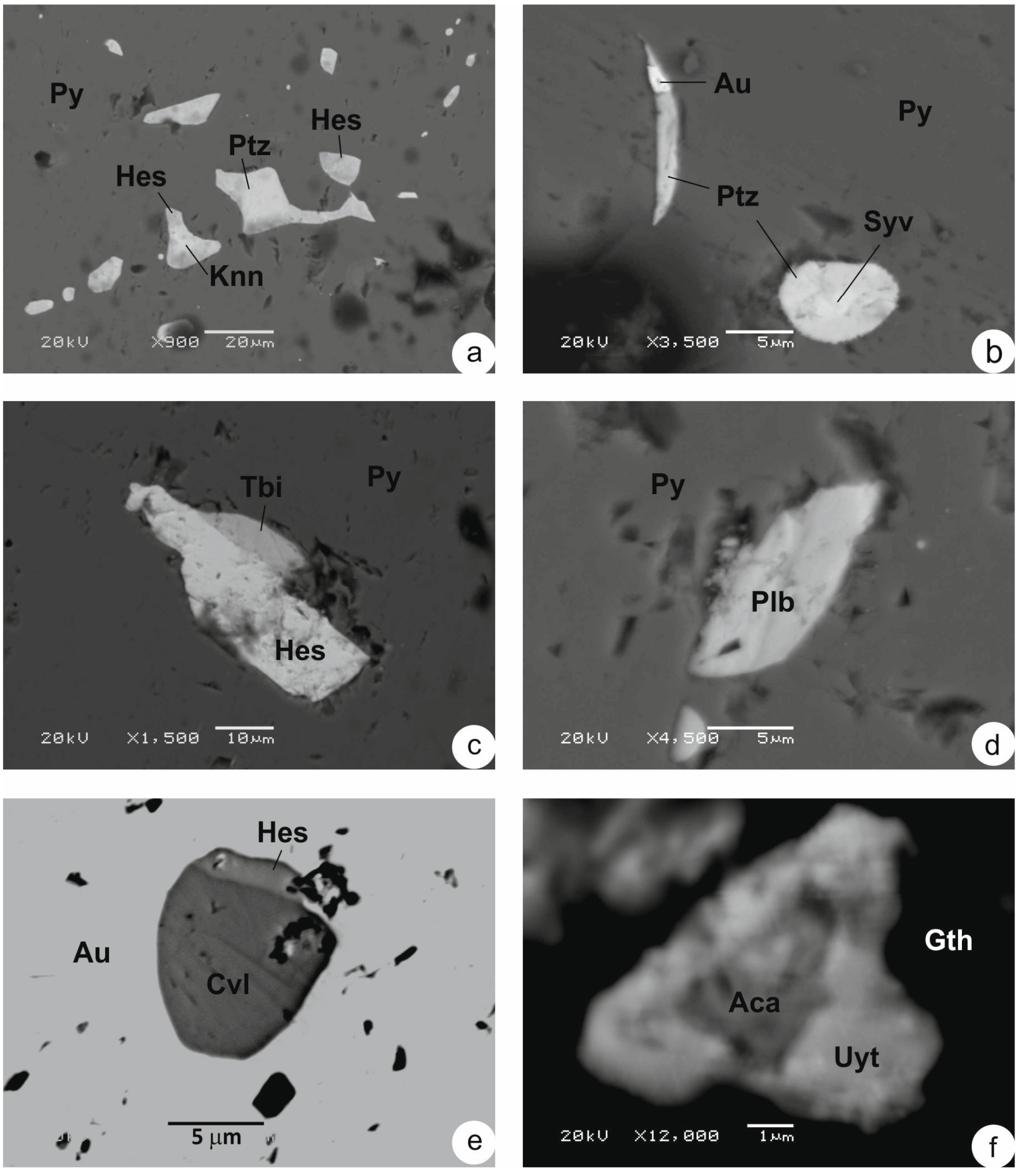

Figure 4. Gold–silver–telluride mineralization of the Spokoininsky ore cluster: (**a**,**b**)—paragenesis of krennerite (Knn), sylvanite (Syv), petzite (Ptz), hessite (Hes), and native gold (Au) in pyrite (Py), (**c**)—jointing of hessite (Hes) and tellurobismuthite (Tbi), (**d**)—polybasite (Plb) in pyrite (Py), (**e**)—cervelleite (Cvl) with hessite (Hes) in supergene gold (Au), (**f**)—acanthite (Aca) with a border of uytenbogaardtite (Uyt) in iron hydroxides (Gth).

Table 3. Chemical composition of Au, Ag, and Te minerals (in wt.%).

Mineral	Ag	Au	Sb	Te	Cu	As	S	Fe	Total	apfu
Native Ag	99.98								99.98	$Au_{1.00}$
Krennerite	3.71	42.60		52.17				2.41	100.89	$Au_{4.23}Ag_{0.67}Fe_{0.84}Te_{8.00}$
Sylvanite	7.08	28.34		63.08					98.50	$Au_{1.16}Ag_{0.53}Te_{4.00}$
Petzite	43.17	21.71		35.60					100.48	$Ag_{2.87}Au_{0.79}Te_{2.00}$
Hessite	62.33			38.40					100.73	$Ag_{1.92}Te_{1.00}$
Cervelleite	68.23			25.12			5.07		98.42	$Ag_{4.00}Te_{1.25}S_{1.00}$
Cu-rich cervelleite	66.14			24.14	5.92		5.38		101.58	$(Ag_{3.65}Cu_{0.56})Te_{1.13}S_{1.00}$
Polybasite	64.57		6.81		8.36	2.26	16.28	2.26	100.53	$[Fe_{0.88}(Ag_{3.97}.Cu_{1.85})_{5.82}(As_{0.65}Sb_{1.21})_{1.86}S_7][Ag_9CuS_4]$
Uytenbogaardtite	56.45	28.53					11.79	4.33	101.10	$Ag_{2.85}Au_{0.79}Fe_{0.43}S_{2.00}$
Acanthite	88.16						8.12	2.91	99.19	$Ag_{3.23}Fe_{0.21}S_{1.00}$

Uytenbogaardtite Ag_3AuS_2 was found in association with spongy and xenomorphic acanthite particles, less often with native gold in oxidized quartz–feldspar metasomatites (Figures 4f and 5). The matrices for minerals are iron hydroxides replacing pyrite. Uytenbogaardtite is characterized by a variable composition (Table 4). It has iron intake from the matrix.

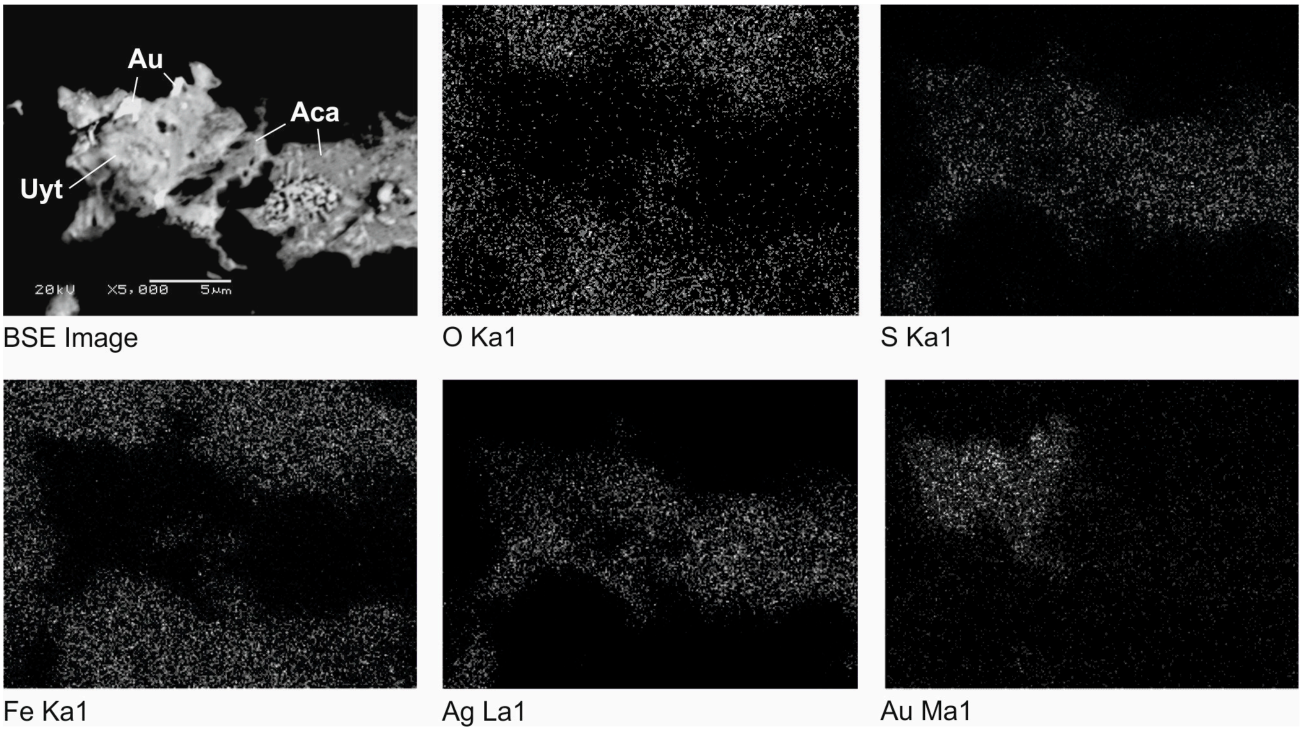

Figure 5. Paragenesis of uytenbogaardtite (Uyt), acanthite (Aca), and native gold (Au) in iron hydroxides: BSE and raster images display the distribution of the elements.

Table 4. Chemical composition of uytenbogaardtite (in wt.%).

No. of Analyses	S	Fe	Ag	Au	Total	apfu
22-5	11.36	6.50	31.66	48.14	97.66	$Ag_{1.66}Au_{1.38}Fe_{0.66}S_{2.00}$
16-5	11.87	4.77	52.14	32.22	101.00	$Ag_{2.61}Au_{0.88}Fe_{0.46}S_{2.00}$
29-1	11.79	4.33	56.45	28.53	101.10	$Ag_{2.85}Au_{0.79}Fe_{0.42}S_{2.00}$
44-3	12.50	3.21	56.15	28.08	99.94	$Ag_{2.67}Au_{0.73}Fe_{0.29}S_{2.00}$
37-2	10.22	3.87	61.92	24.94	100.94	$Ag_{3.60}Au_{0.79}Fe_{0.43}S_{2.00}$
37-1	10.46	4.09	63.71	23.60	101.85	$Ag_{3.62}Au_{0.73}Fe_{0.45}S_{2.00}$

4.2. Typomorphic Features of Gold

Native gold of primary ores and supergene gold of eluvial deposits have been studied.

Granulometry. Native gold in ores is usually finely dispersed and dust-like <5–15 microns, and single grains reach only 0.1 mm.

Supergene gold records the predominance of gold of a very fine fraction (less than <0.1 and 0.1–0.25 mm); medium-sized gold (0.25–0.5 mm) occurs in smaller quantities, and (0.5–1.0 mm) is less common. One small nugget with a size of 5.5 × 3.2 mm was found (Figure 6).

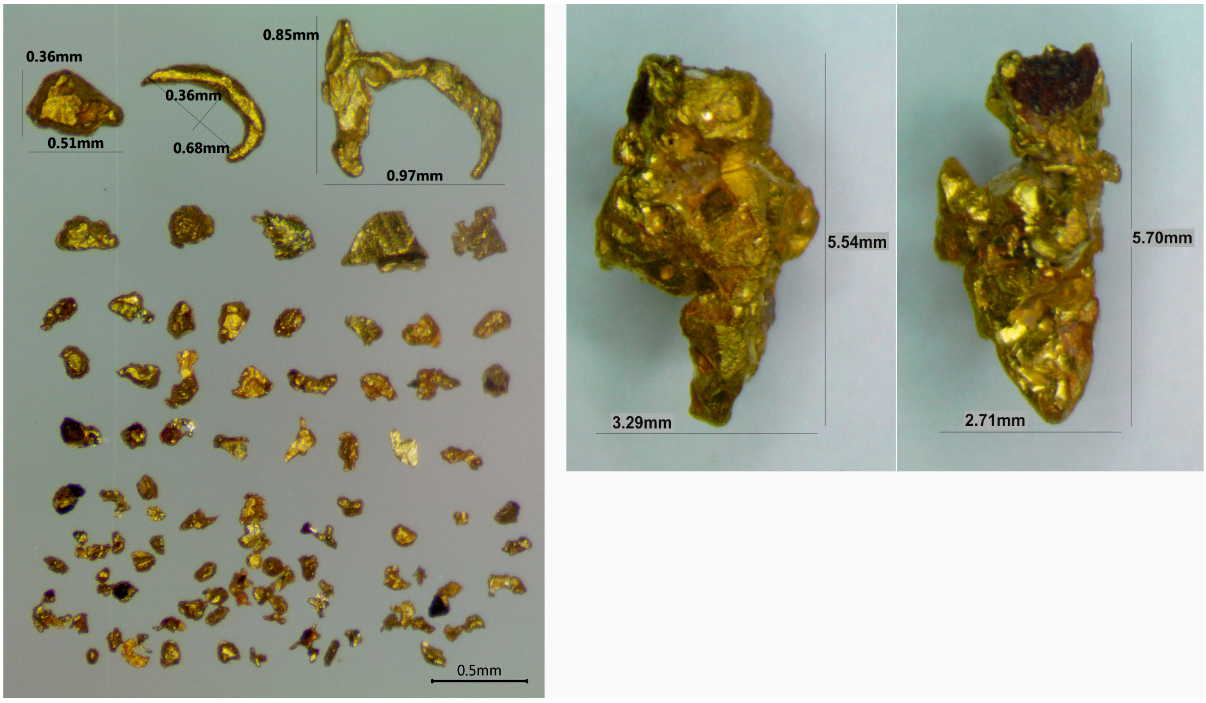

Figure 6. Granulometry of supergene gold.

Morphology. In ores, primary gold has an interstitial and cementing nature. It usually develops in interstices between pyrite grains (Figure 7a) or along cracks in pyrite (Figure 7b), in addition to single pseudoidiomorphic grains of hexagonal appearance (Figure 7c). Microscopically native gold has a porous structure.

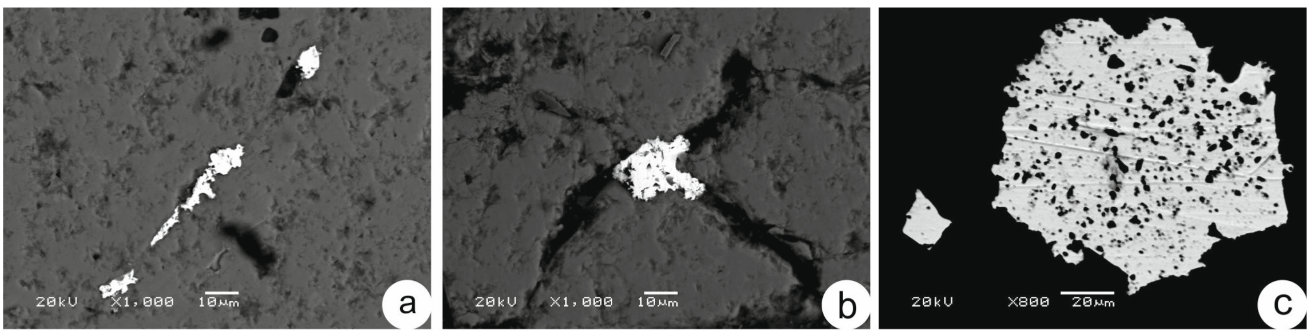

Figure 7. Morphology of native gold of primary ores: (**a**)—interstitial between pyrite grains; (**b**)—cementing along cracks in pyrite; (**c**)—interstitial pseudoidiomorphic grains of hexagonal appearance.

A significant part of supergene gold has a crystalline appearance and is represented by individual crystals or their intergrowths (Figure 8a–e). Crystals form isometric and crystallomorphic grains with shapes close to an octahedron and a combination of a cube and an octahedron, flattened prismatic, elongated needle-like, drusoid, and dendrite-like and coral-like individuals. Striation and growth marks are observed on the crystal faces, and the edges are mostly smoothed. Hemi-idiomorphic gold is also often found—aggregates of grain intergrowths with separate developed cubic and prismatic faces, combined with gold of irregular morphology (Figure 8f). The shape of the grains is of the irregular type, mainly lumpy, scaly, hook-like, lamellar, or wire-shaped (Figure 8h,i). There is a large occurrence of idiomorphic gold in the Mayskoe ore field. In the Spokoinoe ore field, lumpy and scaly gold of irregular morphology was more often observed. Microscopically, gold is usually porous.

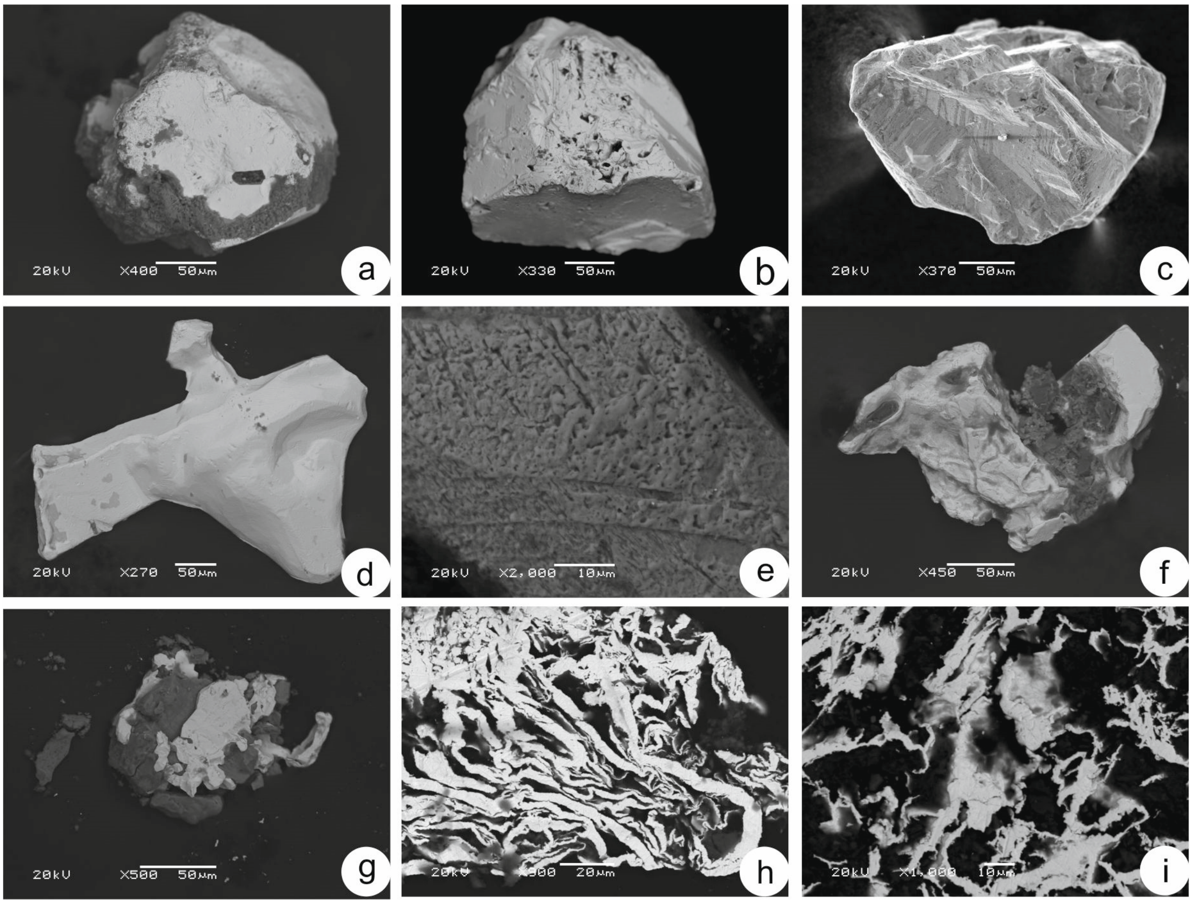

Figure 8. Morphology of supergene gold: (**a**)—isometric crystal of octahedral appearance; (**b**)—isometric crystal with the development of a combination of cube and octahedron shapes; (**c**)—stepped structure of crystallomorphic druzoid gold; (**d**)—clusters of crystals of prismatic and octahedral shapes; (**e**)—prismatic with a microspongy structure; (**f**)—hemi-idiomorphic gold; (**g**)—shell dendritic; (**h**)—lamellar-looped; (**i**)—leafy dendritic.

Often in supergene gold, patterns of the origin of newly formed gold were observed, according to the rhythmiczonal structure of iron hydroxides.

Chemical composition. The main impurity of primary gold according to the microprobe analysis is Ag, and there are single grains with a significant impurity of Cu (6.37–30.04 wt.%). The fineness of native gold has wide variations ranging from 673 to 993‰. In the Spokoinoe field, low-grade gold prevails (average value—753‰); in the Mayskoe field exists medium-grade (average value—810‰) (Figure 9a).

According to the results of the X-ray spectral microanalysis, the content of impurities Zn, As, Hg, Pb, and Sb in supergene gold was below the sensitivity limit (detection). Minor impurities of Fe (up to 0.139 wt.%), Cu (up to 0.231 wt.%), and Bi (up to 0.199 wt.%) were found in single samples. The supergene gold of the Spokoinoe ore field is characterized by low fineness (701‰–800‰) of approximately 60%, and the share of medium-grade gold (801‰–900‰) accounts for 30% (average value—793‰) (Figure 9b). The Mayskoe ore field is dominated by medium-grade gold (800‰–900‰), which accounts for approximately 50% (average value—842‰). Relatively low-grade (700‰–800‰) and high-grade gold (900‰–950‰) amount to 20% and 22%, respectively.

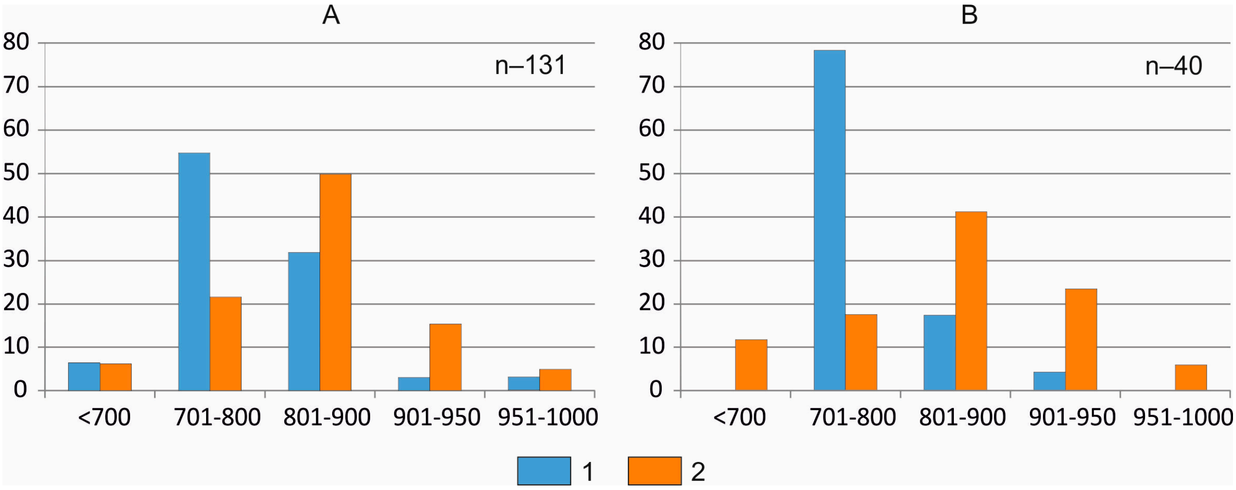

Figure 9. Histograms for the distribution of the fineness of gold: (**A**)—native gold, (**B**)—supergene gold. 1—Spokoinoe ore field, 2—Mayskoe ore field, n—number of analyses.

Compositional heterogeneity. In the same sample, the fineness of primary gold ranges usually from 10 to 130‰, supergene gold usually from 20 to 240‰. Heterogeneous gold, sharply differing in color from bright yellow to a pale whitish color, was identified in shallow-pit samples of the Spokoinoe ore field. Considering morphology, gold is more often thinly lamellar and scaly; in the central part, it has a porous structure, and it is massive on the periphery. The marginal fluctuations of the fineness as a whole are 480‰–999‰ (Figure 10). The overwhelming amount of native gold has a fineness of 750‰–780‰ (average value 778‰). Two types of heterogeneous gold of zonal structure were identified in individual grains. There are gold particles in which the fineness varies from an electrum of 480‰–520‰ on the periphery of the grain to a relatively low-grade 737‰–775‰ in the central parts. Another type of heterogeneous gold is more common—low-grade gold from 668 to 790‰, with a fringe or fragments of a rim of impurity-free native gold. Noteworthy is the complete absence of gold of medium and high fineness in the range 791‰–995‰.

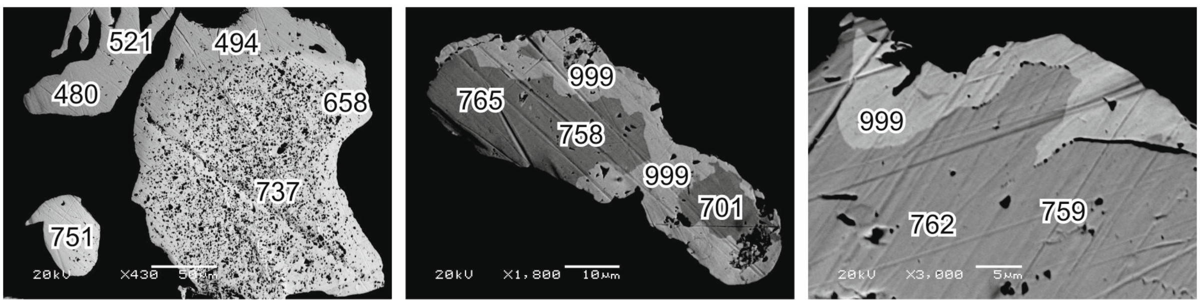

Figure 10. Heterogeneous of supergene gold (the numbers show the degree of fineness).

Relationship with other minerals. Native gold was observed mainly in pyrite and iron hydroxides replacing pyrite and less often in association with hessite, petzite, and acanthite. There is also free gold in quartz and feldspar. In pyrite, native gold is usually located along cracks in the intergranular space or along growth zones. Microporous hessite containing oxygen (Te 28.29–29.90, Ag 54.57–56.75, and O 14.22–16.97) was observed in association with native gold (Figure 11a). Rounded to oval-shaped microinclusions of ore minerals are found in supergene gold: galena, sphalerite, matildite, cuprobismutite, hessite, and cervelleite (Figures 3d, 4e and 11b,c), as well as smirnite from the edge of the grain of gold (Figure 3e). One of the relict grains found in gold is a mixture of hessite and nonequilibrium gold-containing cervelleite-like phase (Te 14.6–27.33, Ag 55.82–59.29, Au 9.97–21.50, and S 3.42–8.62) with microinclusions of cervelleite of stoichiometric composition (Figure 11c). Goethite in the intergrowths with supergene gold often contains an admixture of tellurium up to 2–4 wt.%. In addition, there are cases of location of native gold in supergene minerals similar in composition to plumbojarosite and goethite with rhythmiczonal acanthite threads (Figure 11d).

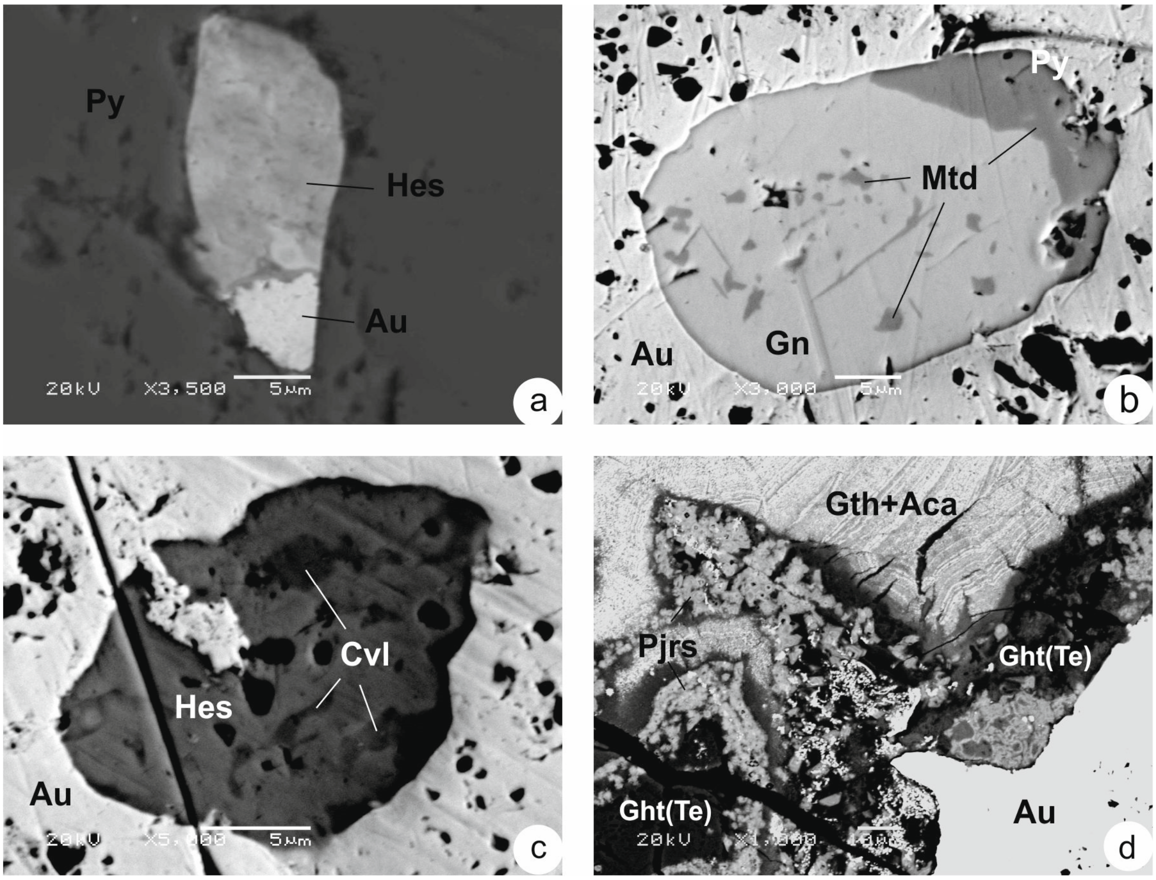

Figure 11. Mineral associations of gold: (**a**)—association of hessite (Hes) and native gold (Au) in pyrite (Py); (**b**,**c**)—relics of minerals in supergene gold: (**b**)—galena (Gn) with phases and border of matildite (Mtd), (**c**)—a mixture of hessite (Hes) with gold-containing cervelleite-like phase and microinclusions of cervelleite (Cvl); (**d**)—the relationship of supergene gold (Au) with plumbojarosite (Pjrs), goethite enriched with tellurium, and goethite with rhythmic-zonal acanthite (Ght + Aca).

5. Discussion

Aldan-Stanovoy gold province is one of the main gold-mining regions in Russia. The gold content of the ASGP is related to hydrothermal–metasomatic processes caused by the Mesozoic tectonic–magmatic activation of the region, involving the intrusion of massifs of subalkaline and alkaline high-potassium igneous rocks of the Jurassic–Cretaceous age [4–11].

The gold mineralization of the ASGP is characterized by a variety of geological and structural positions, hydrothermal–metasomatic formations, and mineral types. Ore-bearing hydrothermal–metasomatic formations are represented by sericite–microcline metasomatites, beresites, gumbaites, jasperoids, and argillizated rocks. The metasomatites of the gumbaite formation are represented by pyrite–carbonate–feldspar metasomatites, which are associated with the main gold and uranium deposits of the Elkon ore cluster. The formation of sericite–microcline metasomatites is associated with the gold–copper–

porphyry (Ryabinovsky) type of mineralization, including veinlet-disseminated sulfide mineralization in alkaline volcano–plutons (Ryabinovoe and Novoe deposits). The jasperoid type of mineralization is represented by deposits formed in three geological structural settings: in contact zones of the Mesozoic alkaline and subalkaline intrusions with carbonate rocks of the Vendian among hydrothermally altered dolomite marbles, magnesian skarns, and syenites (Samolazovsky subtype); in zones of layer-by-layer and intersecting jointing in the Vendian–Lower Cambrian carbonate rocks (Lebedinsky subtype); and at the contact of the Lower Cambrian limestones with the Jurassic sandstones (Kuranakhsky subtype). The gold–argillizite mineralization of the Nimgerkansky type is spatially confined to the intrusions of syenite porphyries of Cretaceous age and is associated with crystal-bearing and amethyst-bearing mineralization. In addition to the Mesozoic mineralization, the Precambrian gold mineralization of the Piniginsky type occurs in the basites of the Medvedev complex [12].

Gold mineralization of the Spokoininsky cluster is represented by a volumetric, nonlinear type, which is unconventional for the region, related to elements of plicative structures and reverse fault tectonics in the enclosing metamorphic basement rocks. Ore zones represent an echeloned system of scalariform deposits grading into gently plunging ore columns in the frontal part of the reverse fault. The connection of gold mineralization with the Mesozoic magmatism is discussed.

For a better understanding of the factors of the formation of gold mineralization, it is necessary to conduct studies of physical–chemical and isotope–geochemical parameters as well as determine the age of mineralization for correlation with magmatic events.

Ore content is related to mineralized zones of crush, cataclase, shear, and schistosity. During the tectonic processing, the porosity of metamorphic and igneous rocks increased, which was a favorable environment for hydrothermal–metasomatic transformations. On the basis of the petrographic study of wallrock changes in igneous and metamorphic rocks and ores of the Spokoininsky cluster, gold-bearing metasomatites can be referred to as low-temperature hydrothermal–metasomatic formations of the beresite and argillized formations. Beresites develop along gneisses and syenites and consist of quartz, sericite, muscovite, hydromica, chlorite, ferruginous carbonates, and fine-grained pyrite. Argillized quartz–feldspar metasomatites are very common in the area of the cluster, often bearing vein–veinlet mineralization of drusoid quartz. The level of gold content is directly dependent on the thickness of wallrock metasomatites and the intensity of silification.

Noble metal mineralization is associated with gold–bismuth (Au-Bi) and gold–silver–telluride (Au-Ag-Te) mineral types.

Gold–bismuth mineralization is locally developed in the deposits of the Aldan shield. Bismuth mineralization has been identified in the ores of deposits close to the Stanovoy plutogenic region in the areas of acidic dikes and small intrusions: Altan-Chaidakh (granodiorites, diorite porphyrites, and dacites) and Bodorono (diorite porphyrites) [13–16]. These deposits, as well as the Spokoininsky cluster, are confined to the zone of the Tyrkanda fault. In addition, bismuth mineralization is developed in the ores of the Lebedinsky cluster located in the center of the magmatogenic structure, where the most intense magmatism occurred in the Central Aldan region. The presence of bismuth mineralization in the ores of the Spokoininsky cluster suggests the influence of acid magma.

The features of the geological structure of the Altan-Chaidakh deposit are determined by the occurrences of the Mesozoic magmatism, very significant in volume and area of distribution, which is related to the Altan-Chaidakh volcanic–tectonic structure. Mineralization is localized in the Lower Jurassic sandstones and the sills of porphyry dacites injecting them. Ore mineralization is represented by complex gold–polymetallic and gold–tellurium–bismuth mineral associations.

Of particular interest are sulfotellurides and tellurides Bi and sulfosalts Pb-Bi, as they are related the groundmass of visible native gold. A wide range of bismuth minerals has been identified, represented by bismuth, tetradymite, bismutoplagionite, bursaite, kosalite, tellurobismuthite, sulfotsumoite, schirmerite, tellurites, and bismuth oxides. Ag, Sb, Cu, and Se are frequent impurities of bismuth minerals. Native gold associated with bismuth minerals has a fineness of 850‰–890‰ [13].

Two producing associations have been identified at the Bodorono deposit: gold–polymetallic and gold–tellurium–bismuth [14–16]. The latter contains lillianite (contains impurities Ag (3.03 wt.%), Sb (1.48 wt.%), and Te (0.52 wt.%)), bismuthite, native bismuth, pilsenite, rare bismuth sulfoselenide, laitakarite (in composition of the mineral, S completely replaced by Se), secondary bismuth mineral smirnite, and tetradymite group minerals—tellurobismuthite, tetradymite, and hedleyite (contains impurity Se (3.72 wt.%)). Native gold with a high fineness of 820‰–940‰ is found in growths with lillianite, bismuthite, and tellurobismuthite.

The predominant spread of both bismuth and telluride mineralization in the area of the Spokoininsky cluster is characterized by the ores of the Mayskoe field. The reason is, apparently, on the one hand, the large granitization of the host complex, the presence of unexposed massifs, as well as a higher hypsometric level of gold mineralization. On the other hand, in the Spokoinoe field, a significant part of the ore bearing the mineralization of Bi and Te underwent denudation, and likely served as a source of placer gold. Secondary bismoclite was observed in the ores, whereas matildite, hessite, and cervelleite were preserved only as relics in supergene gold.

Rare bismuth oxychloride, bismoclite (BiOCl), first described by Mountain (1935), was identified in a sample of eluvial origin, selected on the surface of a pegmatite outcrop at Steinkopf, Namaqualand, Cape Province of South Africa [17]. Subsequently, the bismoclite was identified mainly in the form of alluvial samples near bismuth-containing granite pegmatites or as weathering products of bismuth sulfides in greisen deposits; it was also found in epithermal and volcanic massive sulfide deposits with low and high sulfide content. On the Aldan shield, bismoclite was also found in the Khokhoy karst deposit in the north of the structure, where no other bismuth mineralization was found [18].

The first finding of bismoclite in an ore sample of hydrothermal–magmatic breccia of the San Francisco de los Andes porphyry Bi-Cu-Au deposit, Argentina, is described by [19]. Bismoclite (BiOCl) was found in association with preisingerite ($Bi_3(AsO_4)_2O(OH)$). It is assumed that the bismoclite was formed as a result of weathering of hypogene bismuth-bearing minerals under the influence of meteoric waters containing O_2 and HCl. In addition, the discovery of bismoclite as a mineral phase in the oxidized zone of weathered sediments indicates the existence of hypogene mineralization of Bi at depth.

In our case, bismoclite, along with relic grains of cuprobismutite and matildite, is most likely evidence of the former existence of bismuth mineralization in the ores of the Spokoininsky cluster, which played a significant role in the formation of gold.

Telluride mineralization widely occurs in many gold deposits of the Aldan shield, where it is late, superimposed on early pyrite–quartz mineralization. Au-Bi-Te, Au-Ag-Te, and mixed types of telluride mineralization are found in the distribution of which zoning is identified [20]. In the north of the Aldan shield, the Au-Ag-Te type dominates. In the south, the gold mineralization of the Bodorono and Altan-Chaidakh deposits, bearing various bismuth tellurides, is referred to as the Au-Bi-Te type. The ores of the Spokoininsky cluster are characterized by the presence of mixed Au-Bi-Ag-Te mineralization. Bi-Te minerals include tellurobismuthite and smirnite; and Au-Ag-Te includes krennerite, sylvanite, hessite, petzite, and cervelleite. The existing cases of close growth of tellurobismuthite and hessite are evidence of their paragenetic relationship. While hessite, petzite, and tellurobismuthite are common minerals of the tellurium of the Aldan shield, gold tellurides of the krennerite group are found in a limited number of deposits, and cervelleite is found only in the ores of the Spokoininsky cluster. It was identified as a relict inclusion in supergene gold in association with hessite.

Cervelleite is found in ores of various deposits, including volcanogenic Bambolla mine, Moctezuma, Sonora, (Mexico) (the first finding) [21], Um Samiuki, Egypt [22], deposits of the Southern Urals [23], porphyry San Martin deposit, Argentina [24], Funan Au deposit, China [25], epithermal Mayflower Au-Ag deposit, Montana [26], Eniovche, Bulgaria [27], Larga, Roşia Montană, Romania [28,29], and skarn Băiţa Bihor and Ocna de Fier, Romania [28,29]. That is, they were identified in ore systems that were genetically related to magmatism.

Cervelleite of the Spokoininsky cluster is characterized by a stable admixture of copper up to 5.92 wt.%. It is not uncommon; a similar cervelleite rich in Cu (up to 6 wt.% Cu) is reported in several works [22,23,30]. On the basis of wide variations in the composition and physical properties of cervelleite-like sulfotellurides, Novoselov et al. (2006) [23] suggest the existence of several new phases which can be distinguished by the Cu content, Te/S ratios, and, presumably, by the crystal structure.

Uytenbogaardtite Ag_3AuS_2 is a rare sulfide of gold and silver. Its formation is possible both in hypogene [31–34] and supergene [35–38] conditions. Uytenbogaardtite of the Spokoininsky cluster has a clearly hypergene nature of formation, as it was identified in association with acanthite in the oxidation zone of quartz–feldspar ore metasomatites. The matrix for minerals is iron hydroxide replacing pyrite, and the chemical composition of uytenbogaardtite is characterized by significant dispersion, which can be explained by the nonequilibrium medium of its formation present in supergene conditions.

The analysis of the obtained data on primary and supergene gold showed the enlargement of gold and the appearance of crystalline forms in eluvial deposits. At the same time, there is a tendency to refine gold, but not to a significant extent. Characteristic edges of pure gold were observed locally. The reason for this was a small degree of oxidation of gold; relics of sulfides were preserved in it.

The difference in the fineness of native gold in the Mayskoe and Spokoinoe ore fields was revealed. Different mineral types are characterized by different typochemistry of native gold. The development of gold–rare-metal mineralization in the Mayskoe ore field explains the higher fineness of native gold. Low-grade gold is characteristic of ores bearing gold–silver–telluride association.

The association of native gold with minerals of tellurium and bismuth minerals indicates their paragenetic relationship. The great importance of bismuth and tellurium mineralization in the formation of gold mineralization has been considered and experimentally proved by many researchers [39–47]. In particular, the model of Au enrichment via the liquid bismuth collector mechanism and Bi/Te control of gold mineralization processes in the study is shown in [39–42], and the substitution of Au-Ag tellurides with native gold in the process of dissolution–reprecipitation is shown in experiments [43–47].

6. Conclusions

The gold mineralization of the Spokoininsky cluster is represented by a volumetric, nonlinear type, which is unconventional for the region, and is related to elements of plicative structures and reverse fault in the enclosing metamorphic basement rocks. Veinlet-disseminated sulfide–(pyrite)–quartz ores form deposit-like bodies in beresites by gneisses and granite gneisses and are related to the Mesozoic igneous rocks of sub-alkaline formations. Noble metal mineralization is characterized by polysulfide (Fe-Cu-Pb), gold–bismuth (Au-Bi) and gold–silver–telluride (Au-Ag-Te) mineral types. Different mineral types have their own typomorphic minerals and typochemistry (fineness and impurities) of native gold.

The widespread distribution of telluride mineralization and its great importance in the formation of gold mineralization on the Aldan shield is confirmed. The distribution area of bismuth (including tellurium–bismuth) mineralization in the southern part of the Aldan shield, in the zone of influence of the Stanovoy deep fault, has been identified.

The conducted mineralogical and geochemical studies show a large commercial prospect of the Mayskoe ore field, less affected by denudation processes, in contrast to the ores of the Spokoinoe ore field, which serve as a source of rich gold-bearing placers.

Author Contributions: Conceptualization, methodology, data curation, and writing—original draft preparation, L.A.K. and G.S.A.; writing—review and editing, L.A.K.; fieldwork, investigation, and visualization, L.A.K. and V.N.K. All authors have read and agreed to the published version of the manuscript.

Funding: This work was supported by the Diamond and Precious Metal Geology Institute, Siberian Branch of the Russian Academy of Sciences (DPMGI SB RAS).

Acknowledgments: We thank N. Khristoforova and S. Karpova for assistance with the SEM analysis (Diamond and Precious Metal Geology Institute, Siberian Branch of the Russian Academy of Sciences). We thank E. Sokolov from JSC "Yakutskgeologiya" for his input in the original work, for the organization of field work, and for his contributions to Figures 1 and 2. We also thank all the editors and anonymous referees.

Conflicts of Interest: The authors declare no conflict of interest.

References

1. Sokolov, E.P.; Babkina, T.G.; Makogonov, I.V.; Linnik, I.A.; Khalgaev, E.U.; Shmatkova, L.E.; Anisimova, G.S.; Kondrat'eva, L.A.; Kardashevskaia, V.N. A new type of gold mineralization in the basement of the Aldan-Stanovoi gold-bearing province. *Ores Met.* **2022**, *2*, 122–140. [CrossRef]
2. Burakov, L.F.; Verevkin, N.I.; Vinichuk, L.Y.; Gomzikov, B.A.; Plotnikov, O.I.; Dik, I.P.; Kalinin, Y.A.; Kolosov, N.P.; Komogortsev, G.P.; Korol'kov, A.P. *Report on Geological Survey Field Works on a Scale of 1:50.000 in the Tyrkandinsky Ore District for 1971–1973*; 1974; Unpublished work.
3. Folomkina, V.A. *Report on the Results of the Detailed Exploration of the a Placer Gold Deposit in the Upper Reaches of the River Bolshaya Tyrkanda for 1991–1996 with Inventory Count*; 1996; Unpublished work.
4. Vetluzhskikh, V.G.; Kim, A.A. Geological and commercial types of gold deposits in Southern Yakutia. *Otechestvennaya Geol.* **1997**, *1*, 16–24.
5. Ugriumov, A.N.; Dvornik, G.P. Altered Formations and Gold Mineralization in the Ore Region of the Mesozoic Tectonic-Magmatic Activation (Aldan Shield). Izvestiya of the Ural State Mining and Geological Academy. *Geol. Geophys. Ser.* **2000**, *10*, 119–128.
6. Vetluzhskikh, V.G.; Kazansky, V.I.; Kochetkov, A.Y.; Yanovskiy, V.M. Central Aldan gold deposits. *Geol. Ore Depos.* **2002**, *44*, 467–499.
7. Kazansky, V.I. The unique Central Aldan gold-uranium ore district (Russia). *Geol. Ore Depos.* **2004**, *46*, 195–211.
8. Kochetkov, A.Y. Mesozoic gold-bearing ore-magmatic systems of the Central Aldan. *Russ. Geol. Geophys.* **2006**, *47*, 850–864.
9. Boitsov, V.E.; Pilipenko, G.N.; Dorozhkina, L.A. Gold and gold-uranium deposits of Central Aldan. In *Proceedings of the Large and Superlarge Deposits of Ore Minerals*; Strategic Types of Ore Raw Materials; IGEM RAS: Moscow, Russia, 2006; Volume 2, pp. 215–240.
10. Maksimov, E.P.; Uyutov, V.I.; Nikitin, V.M. The Central Aldan gold-uranium ore magmatogenic system, Aldan-Stanovoy shield, Russia. *Russ. J. Pac. Geol.* **2010**, *4*, 95–115.
11. Dvornik, G.P. Gold-ore metasomatic formations of the Central Aldan region. *Lithosphere* **2012**, *2*, 90–105.
12. Kravchenko, A.A.; Smelov, A.P.; Berezkin, V.I.; Popov, N.V. *Geology and Genesis of Precambrian Gold-Bearing Metabasites of the Central Part of the Aldano-Stanovoy Shield (on the Example of the P. Pinigin Deposit)*; Ofset: Yakutsk, Russia, 2010; 147p.
13. Anisimova, G.S.; Sokolov, E.P. Altan-Chaidakh—Promising object of the Southern Yakutia. *Otechestvennaya Geol.* **2015**, *5*, 3–10.
14. Anisimova, G.S.; Sokolov, E.P. The Bodorono deposit—New gold ore object of the Southern Yakutia. *Ores Met.* **2014**, *5*, 49–57.
15. Anisimova, G.S.; Sokolov, E.P.; Kardashevskaya, V.N. Gold-rare-metal (Au-Mo-Te-Bi) mineralization of the Upper-Algominsky gold-bearing region (Southern Yakutia). *Otechestvennaya Geol.* **2017**, *5*, 12–22.
16. Kardashevskaya, V.N. *Gold Mineralization of the Algominsky Ore Node of the South Aldan Metallogenic Zone: Mineralogy and Conditions of Ore Formation//ABSTRACT of Thesis for the Degree of PhD in Geological Sciences*; Ofset: Novosibirsk, Russia, 2022; 25p.
17. Mountain, E.D. Two new bismuth minerals from South Africa. *Mineral. Mag.* **1935**, *24*, 59–64. [CrossRef]
18. Kondratieva, L.; Anisimova, G. Minerals of Hg, Tl and As of Khokhoy Deposit (Aldan Shield). In Proceedings of the Geology and Mineral Resources of the North-East of Russia: Materials of the XII All-Russian Scientific and Practical Conference Dedicated to the 65th Anniversary of the Institute of Geology of Diamond and Precious Metals, Siberian Branch of the Russian Academy of Sciences, Yakutsk, Russia, 23–25 March 2022; pp. 184–188.
19. Testa, F.J.; Cooke, D.R.; Zhang, L.; Mas, G.R. Bismoclite (BiOCl) in the San Francisco de los Andes Bi-Cu-Au Deposit, Argentina. First Occurrence of a Bismuth Oxychloride in a Magmatic-Hydrothermal Breccia Pipe and Its Usefulness as an Indicator Phase in Mineral Exploration. *Minerals* **2016**, *6*, 62. [CrossRef]
20. Kondratieva, L.A.; Anisimova, G.S.; Kardashevskaia, V.N. Types of Tellurium Mineralization of Gold Deposits of the Aldan Shield (Southern Yakutia, Russia). *Minerals* **2021**, *11*, 698. [CrossRef]
21. Criddle, A.J.; Chisholm, J.E.; Stanley, C.J. Cervelleite, Ag_4TeS, a new mineral from the Bambolla mine, Mexico, and a description of a photo-chemical reaction involving cervelleite, acanthite and hessite. *Eur. J. Miner.* **1989**, *1*, 371–380. [CrossRef]

22. Helmy, H.M. The Um Samiuki volcanogenic Zn-Cu-Pb-Ag deposit, Eastern Desert, Egypt: A possible new occurrence of cervelleite. *Can. Miner.* **1999**, *37*, 143–158.
23. Novoselov, K.A.; Belogub, E.V.; Zykov, V.V.; Yakovleva, V.A. Silver sulfotellurides from volcanic-hosted massive sulphide deposits in the Southern Urals. *Mineral. Petrol.* **2006**, *87*, 327–349. [CrossRef]
24. Paar, W.; De Brodtkorb, M.K. *Presencia de Cervelleíta y Hessita en la Galena del Yacimiento San Martín, Valcheta, Provincia. de Río Negro. 3° Reunión de Mineralogía y Metalogenia, Instituto de Recursos Minerales*; Universidad Nacional de La Plata, Argentina Publicación 5: Buenos Aires, Argentina, 1996; Volume 5, pp. 173–175.
25. Gu, X.P.; Watanabe, M.; Hoshino, K.; Shibata, Y. New find of silver tellurosulphides from the Funan gold deposit, East Shandong, China. *Eur. J. Miner.* **2003**, *15*, 147–155. [CrossRef]
26. Spry, P.G.; Thieben, S.E. Two new occurrences of benleonardite, a rare silver tellurium sulphosalt, and a possible new occurrence of cervelleite. *Miner. Mag.* **1996**, *60*, 871–876. [CrossRef]
27. Dobrev, S.; Strashimirov, S.; Vassileva, M.; Dragiev, H. *Silver and Silver-Bearing Phases from Chala and Pcheloiad Deposits (Eastern Rhodopes) and Eniovche Deposit (Central Rhodopes)*; Annual of the University of Mining and Geology 'St. Ivan Rilski': Sofia, Bulgaria, 2002; Volume 45, pp. 39–44.
28. Cook, N.J.; Ciobanu, C.L. Cervelleite, Ag_4TeS, from three, localities in Romania, substitution of Cu, and the occurrence of the associated phase, Ag_2Cu_2TeS. *N. Jb. Miner. Mh.* **2003**, *7*, 321–336. [CrossRef]
29. Ciobanu, C.L.; Cook, N.J.; Tămaş, C.; Leary, S.; Manske, S.; O'Connor, G.; Minuţ, A. Tellurides-Gold-Base Metal Associations at Roşia Montană: The Role of Hessite as Gold Carrier. In *Au-Ag-Telluride Deposits of the Golden Quadrilateral, South Apuseni Mountains, Romania*; Cook, N., Ciobanu, C.L., Eds.; IAGOD Guidebook Series; Natural History Museum of Landon: London, UK, 2004; Volume 12, pp. 187–202.
30. Voudouris, P.; Spry, P.G.; Sakellaris, G.A.; Mavrogonatos, C. A cervelleite-like mineral and other Ag-Cu-Te-S minerals [Ag_2CuTeS and $(Ag, Cu)_2TeS$] in gold-bearing veins in metamorphic rocks of the Cycladic Blueschist Unit, Kallianou, Evia Island, Greece. *Miner. Petrol.* **2011**, *101*, 169–183. [CrossRef]
31. Nekrasov, I.Y. *Geochemistry, Mineralogy and Genesis of Gold Lodes*; Nauka: Moscow, Russia, 1991; 302p. (In Russian)
32. Warmada, I.W.; Lehmann, B.; Simandjuntak, M. Polymetallic sulfides and sulfosalts of the Pongkorepithermal gold-silver deposit, West Java, Indonesia. *Can. Miner.* **2003**, *41*, 185–200. [CrossRef]
33. Pal'yanova, G.A.; Savva, N.E. Specific genesis of gold and silver sulfides at the Yunoe Deposit (Magadan Region, Russia). *Russ. Geol. Geophys.* **2009**, *50*, 587–602. [CrossRef]
34. Pal'yanova, G.A.; Kokh, K.A.; Seryotkin, Y.V. Formation of gold and silver sulfides in the System Au-Ag-S. *Russ. Geol. Geophys.* **2011**, *52*, 443–449. [CrossRef]
35. Barton, M.D.; Kieft, C.; Burke, E.A.J.; Oen, I.S. Uytenbogaardtite, a new silver-gold sulfide. *Can. Miner.* **1978**, *16*, 651–657.
36. Castor, S.B.; Sjoberg, J.J. Uytenbogaardtite, Ag_3AuS_2, in the Bullford mining district, Nevada. *Can. Miner.* **1993**, *31*, 89–98.
37. Greffié, C.; Bailly, L.; Milési, J.-P. Supergene alteration of primary ore assemblages from low-sulfidation Au-Ag epithermal deposits at Pongkor, Indonesia, and Nazareño, Perú. *Econ. Geol.* **2002**, *97*, 561–571. [CrossRef]
38. Savva, N.E.; Pal'yanova, G.A. Genesis of gold and silver sulfides at Ulakhan deposit (northeastern Russia). *Russ. Geol. Geophys.* **2007**, *48*, 799–810. [CrossRef]
39. Ciobanu, C.L.; Cook, N.J.; Pring, A. Bismuth Tellurides as Gold Scavengers. In *Mineral Deposit Research: Meeting the Global Challenge*; Mao, J.W., Bierlein, F.P., Eds.; Springer: Berlin, Germany, 2005; pp. 1383–1386.
40. Tooth, B.; Brugger, J.; Ciobanu, C.L.; Liu, W. Modelling of gold-scavenging by bismuth melts coexisting with hydrothermal fluids. *Geology* **2008**, *36*, 815–818. [CrossRef]
41. Douglas, N.; Mavrogenes, J.; Hack, A.; England, R. The Liquid Bismuth Collector Model: An Alternative Gold Deposition Mechanism. In Proceedings of the 15th Australian Geological Congress Abstracts, Sydney, NSW, Australia, 3–7 July 2000; Volume 59, p. 135.
42. Feng, H.; Shen, P.; Zhu, R.; Tomkins, A.G.; Brugger, J.; Ma, G.; Li, C.; Wu, Y. Bi/Te control on gold mineralizing processes in the North China Craton: Insights from the Wulong gold deposit. *Miner. Depos.* **2023**, *58*, 263–286. [CrossRef]
43. Zhao, J.; Pring, A. Mineral Transformations in Gold—(Silver) Tellurides in the Presence of Fluids: Nature and Experiment. *Minerals* **2019**, *9*, 167. [CrossRef]
44. Zhai, D.; Liu, J. Gold-telluride-sulfide association in the Sandaowanzi epithermal Au-Ag-Te deposit, NE China: Implications for phase equilibrium and physicochemical conditions. *Miner. Petrol.* **2014**, *108*, 853–871. [CrossRef]
45. Zhao, J.; Brugger, J.; Xia, F.; Ngothai, Y.; Chen, G.; Pring, A. Dissolution-reprecipitation vs. solid-state diffusion: Mechanism of mineral transformations in sylvanite, $(AuAg)_2Te_4$, under hydrothermal conditions. *Am. Miner.* **2013**, *98*, 19–32. [CrossRef]
46. Zhao, J.; Brugger, J.; Grundler, P.V.; Xia, F.; Chen, G.; Pring, A. Mechanism and kinetics of a mineral transformation under hydrothermal conditions: Calaverite to metallic gold. *Am. Miner.* **2009**, *94*, 1541–1555. [CrossRef]
47. Xu, W.; Zhao, J.; Brugger, J.; Chen, G.; Pring, A. Mechanism of mineral transformations in krennerite, Au_3AgTe_8, under hydrothermal conditions. *Am. Miner.* **2013**, *98*, 2086–2095. [CrossRef]